An Optimized Channel Design for Air to Ground Communication Systems

[1]Neethu J Pillai, [2]Poornima B
[1] M.Tech Scholar, [2] Assistant Professor, Electronics and Communication Engineering
[1]Digital Electronics and Communication Engineering,
[1] Atria Institute of Technology, Anandnagar, Bangalore, India

Abstract: Two prominent Future Communication Infrastructure (FCI) applicants that were anticipated recently due to speedy rise in the air traffic volume were the 1-2 GHz band aeronautical frameworks L-DACS1 and L-DACS2 for Air-to-Ground (AG) communication with the most suitable approach being selected as L-DACS1. A filter bank multicarrier (FBMC) based communication systems is been proposed and also its advantages over LDACS systems has been shown in this work. Spectral density of power, Signal to interference rate, and BER execution are the 3 parameters that are used to measure against all future aeronautical communication systems. In the existence of distance measuring equipment (DME) that produces the original obstructing signals, it could be seen that FBMC produces enhanced working when compared with the LDACS proposals. Simulation results show that the presence of well-localized subcarrier prototype filters in the Filter bank multicarrier practically minimizes the out-of-band power and also the obstruction from DME can be reduced. Eliminating CP, postfix and windowing method employed in LDACS and also shortening the number of guard band subcarriers in FBMC could enhance the throughput and spectral efficiency. Thus proving FBMC based communication framework could be an attractive applicant for the imminent air to ground communication entity.

Index Terms **- Bit error rate (BER), Distance measuring equipment (DME), Filter bank multicarrier (FBMC), Future communication infrastructure (FCI), L-band digital aeronautical communication systems (LDACS), Power spectral density (PSD, Signal to interference ratio (SIR).**

I. INTRODUCTION

Transmission of information or power among multiple points that are not linked by an electric wire is called Wireless communication. Radio wave is used by the most common radio-communication technologies. Radio waves could be relatively short meters usually used in television application or to the extent thousands or a large number of kilometers utilized for remote ocean communication which includes mutual radios, personal digital assistants, and remote interconnections. Communication between person on the ground and those in the aeronautical vehicles is known as Air to ground communication. The bands that are suitable for air to ground communication are VHF, L-band as well as S-band. VHF varies from 30-300MHz and their common uses are FM radio transmission, air traffic control communications and air navigation work, whereas L& S-band which is (1-2GHz) and (2-4GHz) respectively and has uses in aircraft surveillance and satellite & space communication respectively .It was required to enhance the airborne communication foundation for managing the air traffic termed as (ATM) & flight control and International Civil Aviation Organization (ICAO) acknowledged it in 2002. The ICAO is in charge of stating and also organizing the technology and radio frequency (RF) spectrum mainly used for aerial communications. Firstly, the improvement made in FCI comprised of 2 agendas : assistance by the European Union i.e., EUROCONTROL for the Single European Sky ATM Research, and the assistance by National Aeronautics and Space Administration which was administered by US Federal Aviation Administration for the Next Generation Air Transportation System (NextGen). Two systems fusion guaranteed continental aeronautical communication that was employed in very high frequency (VHF) band. The first system being analog system that succeeded for communication of voice that has been used for beyond 50 years. Newly developed digital system that permits data communication is the second system. Present aviation communication systems were inadequate to hold on the air traffic rise, this caused to the development of new demands with high data rates links. Advancement on the current aeronautical communication (VHF) systems was introduced but it was found that not a single system could deliver ever-lasting solutions, not even after 2020.

As there will be a severe increase in air traffic volume in the coming future which implies that the present aerial communication system functioning at VHF will undergo drastic crowding. Depending upon the openness to the existing range air to ground communication systems are to be developed. During the near future when air traffic volume rises, it is anticipated that upcoming communication entities shall be utilized in 960-1164MHz specifically L-band allotted under the aegis of ITU which is more appropriate for aeronautical radio transmission. EUROCONTROL suggested two LDACS systems- LDACS1 and L-DACS2 as the dual FCI applicants. During the hunt for better transmission scenario, research workers started taking other modulation formats into account and one among them is filter bank multicarrier (FBMC). This advanced air to ground communication systems has nearly the same physical layer norms as L-DACS1. Any system being developed has to succeed in dealing with challenges in the future development process and also satisfy the rise in air traffic constantly.

II. L-BAND COMMUNICATION SYSTEM

The figure 1 shows the pictorial representation of L-band communication systems with the existing L-band system being the DME/VOR and the future L-band communication systems being the L-DACS and FBMC (Filter bank multicarrier systems). Due to the overcrowding of the signals in the VHF, it becomes a necessity to develop a new AG communication system in the available spectrum. So, any future aeronautical system that is proposed for future air to ground communication has to operate with less interference with the existing system in that particular band (L-band).

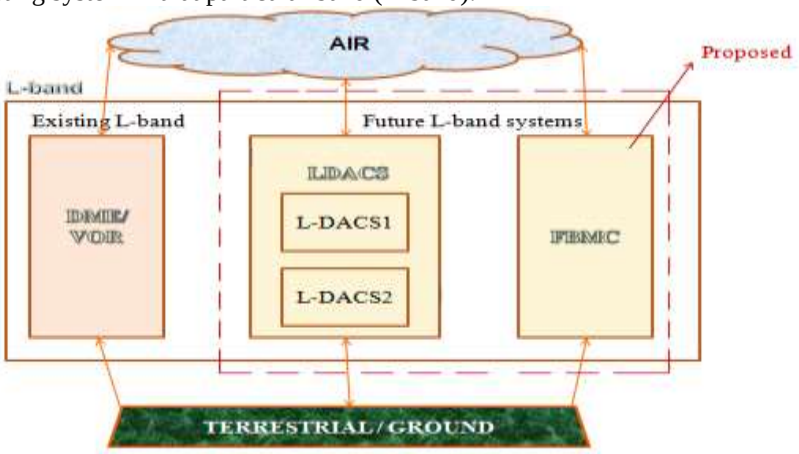

Figure 1: L-band communication sytems

2.1 Existing L-band systems

L-band spectrum and the transmission as well as the pilotage systems that are allotted in the L-band should co-occur with any proposed L-DACS systems have been explained. Figure 2 shows present communication system in L-band.

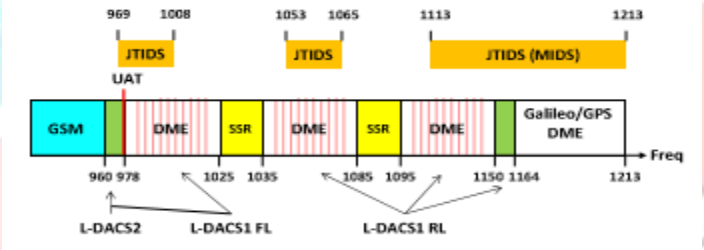

Figure 2: L-band spectrum utilization.

The present DME system was determined to assign the L-DACS channels in an inlay process. From the figure it is found that DME signals occupied the vital fragments of the L-band spectrum. These signals had main applications in radio navigation function. Secondary transponder systems called as legacy systems can be seen in the Figure 4.4 such as Axillary Surveillance Radar (SSR), Universal access transmitter-receiver (UAT), Galileo/GPS, and Joint Tactical Data Distribution System/ Multifunctional Information Distribution System (JTIDS/MITS). Whichever advanced future communication infrastructure entity is proposed should interact with all these existing legacy entities. For aviation security, the Future communication Infrastructure applicant systems must produce least interference to these current systems as well as function in the existence of interference from all these systems. DME is considered to be major distorting signal to the L-band communication system as it is considered to be the most important entity in this region and is in near proximity to the FCI frequencies.

2.2 DME Signal Model

DME is transponder-centered radio route machinery that computes the tilt distance by scheduling propagation lag with respect to signals from L-band. Distance measuring equipment operates in 960-1215MHz band. DME ground units are distributed in a large scale for a geographical area, same as concepts of cellular structure. DME is produced using Gaussian like pulses. Every DME base station transfers series of signal pulse pair as defined in (1). Duo signal is,

$$S_{pulse_{pair}}(t) = e^{-\alpha t^2/2} + e^{\frac{-\alpha t^2 - \alpha \Delta^2 t^2 + 2\alpha \Delta t}{2}} \quad (1)$$

here $\alpha = 4.5 \times 10^{11} s^{-2}, \Delta t = 12 \times 10^{-6} s$

α is said to be a constant that decides the pulse width. Every DME signal is separated by Δt which is a chain of Gaussian shaped pulses pairs. Figure 3 displays time domain single DME signal pulse pairs. DME wave spectrum's following Fourier Transformation,

$$S_{pulse_{pair}}(f) = A\sqrt{\frac{8\Pi}{\alpha}} e^{\frac{(-2\Pi^2 f^2)}{\alpha}} \quad (2)$$

here A value has been particularized depending upon on the DME power states. From evaluation of equation (2), the DME series spectrum is as shown in the figure 4.6 for channel bandwidth 1MHz. In order to produce the DME power spectral density, series of DME pulses are considered from the equation (1). These pulses are shaped based upon the Poisson process. 2700 pulse pairs per second (ppps) are considered for the simulation purposes here in the ground to air scheme.

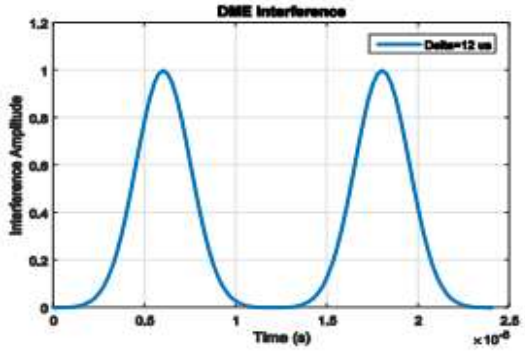

Figure 3: A pair of time domain DME pulse

It is considered that the received signal consists of signals from N_I DME base station moving in the identical / non-identical DME channels. For a given time interval, the signal sequence carried by the i[th] distance measuring equipment base station is given as $N_{i,u,\ u=0,1,2,\ldots\ldots\ldots,M_{i-1}}$ pulse couple, where M_i is the entire amount of pulse duo in the i[th] DME station signal chain.

Poisson process usually displays the casual nature of pulse duo of DME, due to this it is been used in creating of $N_{i,u}$ pulse pair's starting time i.e., $t_{i,u\ \ u=0,1,2\ldots\ldots\ldots M_{i-1}}$. At the receiver the generated and combined DME interfering signal is,

$$i(t) = Real\left(\sum_{i=0}^{N_I}\sum_{u=0}^{M_{i-1}} A_i^{DME}\, S_{pulse_{pair}}(t - t_{i,u}) e^{j2\Pi f_{c,i}t + j\Phi_{i,u}}\right) \quad (3)$$

where $\Phi_{i,u}$ is phase that is evenly transmitted for [0,2Π] interval. For all L-band receiver the cumulative passband DME signals is displayed in equation 3). The acquired DME signal is evaluated by summing up each set of two DME pulse ($N_{i,u,\ u=0,1,2,\ldots\ldots\ldots,M_{i-1}}$) from every distance measuring equipment stations ($i = 0: N_{I-1}$) and by presuming that all L-band receiver consists of N_I DME stations. For all pulse pair the obtained DME signal peak amplitude is

$$A_i^{DME} = \sqrt{\Psi_i^{DME}}, i0,1, \ldots\ldots N_{I-1}, \quad (4)$$

here Ψ_i^{DME} is determined from Friis transmission equation as shown below and indicates the i[th] DME received peak power signal.

$$\Psi_i^{DME} = P_I^i G_{GS}^i(EL^i) L_{free}^i G_{air}^i(-EL^i) \quad (5)$$

here P_I^i indicates peak power of transmitted DME, which takes value as high as 1kWEIRP calculated as the difference between transmitter power and cable losses along with addition of antenna gains.G_{GS}^i represents the ground speed antenna gain of the aircraft at elevation angle EL^i , $G_{air}^i(-EL^i)$ specifies aircraft gain of antenna at $-EL^i$ elevation angle and L_{free}^i defines path depletion in free space. It is found that almost 99% of the DME energy that is been transmitted will be inside the range $\pm$400KHz center frequency of channel. As specified earlier, DME sends 2700 ppps and its redundancy pace confines form 5 to 150 ppps for determining and estimating the signals.

The peak power of the DME GS transmitter takes value between 100W to 1000W, at the same time for a hefty jet aircraft the value is 300W and for a comparatively tiny aircraft needs 100W, for a drone the power required will be lesser. Since L-DACS transmits much lesser power of 10W when compared to the DME transmitting signal, the FCI systems may experience interference from DME in a remarkable manner. From the literature survey it was seen that the DME interference can be lessen in the L-DACS1 by applying pulse blanking (PB) method. Pulse blanking is a technique used to encounter the pulsed interference from either keeping it vacant or nulling-out receiver samples that surpass limit and is by now enforced in E5 and L5 region applied in spacecraft navigation framework. Since the PB method nulls the required signal, the threshold has to be chosen for acceptable signal impairment which is considered to be disadvantage of PB. Insignificant errors will be offered from DME signals as far as the FCI transmit signals are restricted to 10W.

2.3 FCI Candidate Systems In L-Band for Aeronautical Communication

A detailed explanation of the L-DACS systems as well as the recent FBMC aeronautical communication systems in its technical terms is been given in this segment A concise comparison of the physical layer characteristics of all communication systems is discussed.

2.3.1 LDACS1

L-DACS1 is same as that of IEEE 802.16 wireless technologies, which is extensively used in wireless networks. L-DACS1 uses duplexing based on frequency (FDD) which exploits Cyclic prefix – orthogonal frequency division multiplexing

modulation, which assists concurrent transfer of information from land to space channels i.e., forward link (FL) and air to ground i.e., reverse link (RL). Adaptive coding and modulation (ACM) is the method that gives assistance to the data channel in L-DACS1. It is observed that after applying forward error correction (FEC) in LDACS1, at the power level the BER measurement will be not much than 10^{-6}that signifies to the receiver sensitivity. Presently suggested L-DACS1 range is 985.5-1008.5 MHz for forward communication and 1048.5-1071.5 MHz for reverse communication. A difference of 40 MHz acts as a duplex transition area. Star topology is considered in L-DACS1. Frequency domain OFDM subcarriers for forward link structure as shown in the figure 4.

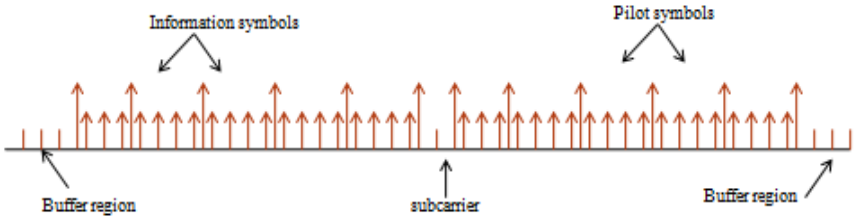

Figure 4: Forward link OFDM subcarriers in frequency domain.

The signal spectrum contains guard bands of 7 and 6 subcarriers to its left and right respectively. When a converse of Fourier transform is applied on this signal for a particular time, it is termed as useful symbol time T_u in time domain. In the discrete domain the replicate of the cyclic prefix$T_{cp}$and $T_w$windowing samples are joined with the useful symbol time before and after respectively. The time domain cyclic prefix (CP) OFDM of L-DACS1 is as shown in the figure 5. T_g contributes to intersymbol interference (ISI) obstruction and blocks synchronization errors for symbol time.

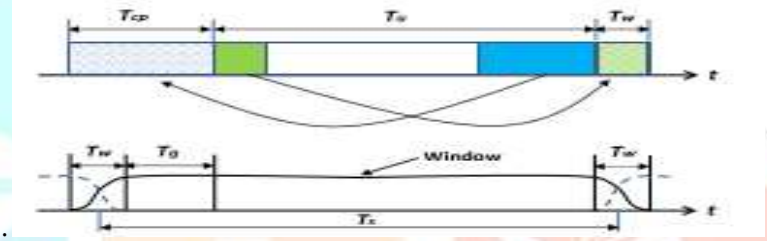

Figure 5: Formation of cyclic prefix-OFDM of L-DACS1.

The core transmission figure of L-DACS1 is as shown in the figure 6. In the frequency domain, 'n' number of subcarriers is individually modulated with complex value. In order to obtain OFDM symbol in time domain a converse Fourier transform operation is done on frequency domain subcarriers. These symbols are fed through the next block which acts as buffer region or a guard interval used for the protection of OFDM symbols from ISI. Transmitter windowing block minimizes the spectral side lobes of OFDM. Complex filtered input is then multiplied by a complex carrier and sent to the channel for transmission. In the reception phase, the converse is performed.

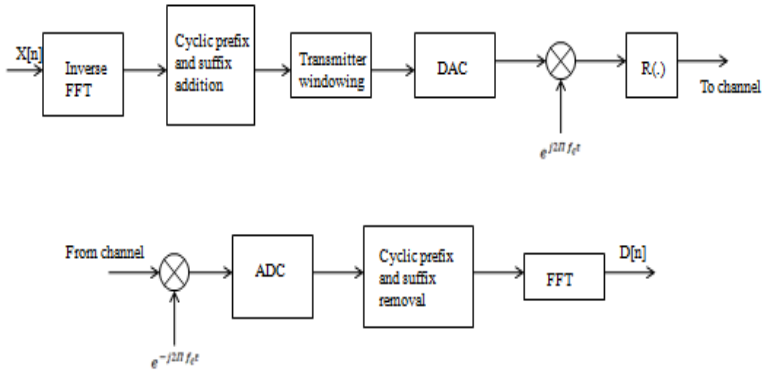

Figure 6: Transceiver block diagram for L-DACS1.

2.3.2 LDACS2

L-DACS2 utilizes GSM approaches and is a individual carrier entity of 200KiloHertzdata transfer capacity which works on duplexing of time technique. The modulation technique used is Gaussian Minimum Shift Keying that divides the accessible spectrum into multiple wide channels. Each bands uses a MSK modulated RF carrier that assists multiple Time Division Multiple Access time slots. Modulation index h is 0.5 and $B_3T$is 0.3 which is a multiplication of 3dB bandwidth B3 and duration of symbol T of the filter. The rate of the symbol can be calculated as 1/T that gives a value of 270.833 ksymbols/s. L-DACS2 frequency is limited to 960-978 MHz lower L-band that is nearer to GSM900 band. Figure 7 describes the core communication system for L-DACS2. Digital signal is transformed into analog using a DAC. These signals are then passed through Gaussian filter which takes care of phase filtering and smooth transitions. A low complexity based differential decoder is used in reception part. The bit decision of the decoder is built on 2 signed multiplications for both even and odd symbols:

$Real(D((n-1))T))\ x\ Imag(D(nT))$ and $Real(D((n-1))T))\ x\ Imag(D(nT))$here D(t) indicates the signal acknowledged following sifting through Gaussian and 'n' indicates the index of sample of discrete time signal.

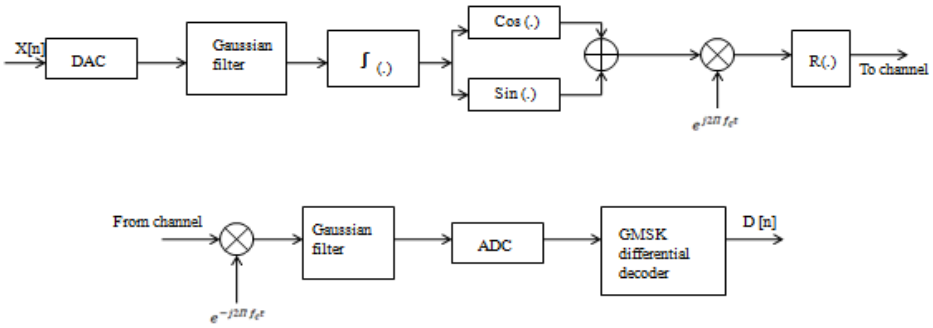

Figure 7: Transceiver block diagram for L-DACS2.

2.3.3 FBMC

Multicarrier communication systems are considered to be the best thriving technique in the field of wireless communication. With a progressive coding as well as modulation schemes, these systems could acquire better spectral efficiency when compared to modulation with single carrier techniques. Filter bank multicarrier system is one of the multicarrier techniques which make use of prototype filters to accomplish a particular objective like reduction of ISI, ICI and stop band energy. The main criteria is to model the prototype filter such that it reduces both inter symbol and inter carrier interferences along with small spectral sidelobes.

The FBMC model that is considered in our project uses staggered multitone (SMT) modulation techniques, as shown in the figure 8. The transmitter part of SMT based FBMC system consists of N subcarrier filters through which N parallel complex data are passed. At the transmitter, each QAM symbols are divided into its in-phase and quadrature parts. Each of them is being time shifted by a symbol period T/2 with respect to one another, this time offset is symbolized by p(t) and p(t-T/2). N subcarrier modulator modulates the result from the filters and these modulators are with carrier spacing of 1/T. This shift of time and frequency for every symbol is called as staggering technique. To meet the orthogonality condition this process becomes a necessity. Another criteria that is required to fulfill right angle condition is to have even as well as symmetric filter p(t) which implies p(t)=p(-t). Because of the closeness to the L-DACS1 characteristics, SMT technique is chosen in our project

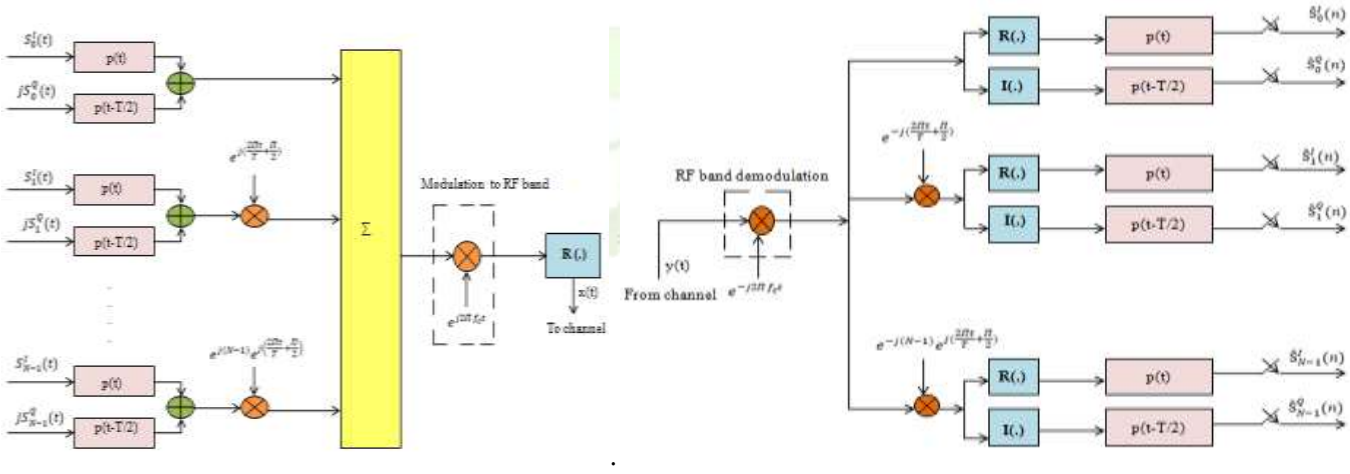

Figure 8: Transceiver block diagram of FBMC.

Continuous signal based on the figure is as shown below,

$$S_k(t) = \sum_n \left(S_k^I[n] + jS_k^Q[n]\right)\delta(t-nT), k = 0,..N-1 \qquad (6)$$

here $S_k[n]$indicates composite valued information in time, $\delta(t)$and k represents Dirac delta function and subcarrier index. The modulated SMT complex valued signal is given as,

$$x(t) = \sum_{k=0}^{N-1} x_k(t) \qquad (7)$$

here $x_k(t)$ is given as,

$$x_k(t) = \sum_n (S_k^I[n]p(t-nT) + jS_k^Q[n]p\left(t-nT-\frac{T}{2}\right))e^{j\left(\frac{2\Pi kt}{T}+\frac{k\Pi}{2}\right)} \qquad (8)$$

The signal accepted by the FBMC receiver along with the interference from the DME is,

$$y(t) = \sum_{m=0}^{N-1} x_m(t) + n + i(t) \quad (9)$$

In equation (9), i(t) indicates values from equation (3) of DME signal and n(t) indicates additive white gaussian noise whose power is estimated from SNR practical. y(t) for m subcarriers are given as,

$$y_m(t) = x_m(t) + n(t) + i(t) \quad (10)$$

On substituting equation (8) in (10), we get the real and imaginary components of the received signal of m subcarriers. Convolution for the prototype filtering is done using real & imaginary term i.e.,

$$Real\left(y_m(t)\right) * p(t), Imag\left(y_m(t)\right) * p(t + T/2)) \quad (11)$$

Values for m subcarrier is obtained by presuming the ideal channel estimation and synchronization and the sampling time for every symbol via prototype filter p(t) is t=nT.

$$\hat{s}_m^I[n] = s_m^I[n] + I_{Real} + n_{Real} \quad (12)$$

$$\hat{s}_m^Q[n] = s_m^Q[n] + I_{Imag} + n_{Imag} \quad (13)$$

here the last 2 terms of both the equations signifies interference from DME and noise in real and imaginary part respectively, where I_{Real} and I_{Imag} are expressed as:

$$I_{Real} = i(t)\cos\left(m\left(\frac{2\Pi t}{T} + \frac{\Pi}{2}\right)\right) * p(t) \quad (14)$$

$$I_{Imag} = i(t)\cos\left(m\left((2\Pi t/T\ + \Pi/2)\right)\right) * p(t + T/2) \quad (15)$$

When judged against L-DACS1 the OOB power of the FBMC in the vicinity of DME frequencies is 80dB less which signifies the neighboring FBMC channels or DME signals has less interference. Subcarrier spacing of FBMC is same as that of L-DACS1. N_{FFT} and Δf indicates FFT size and subcarrier spacing respectively, product of these forms the sum spectrum of these multiple carrier signals. N_u refers to a number of used subcarriers B is the bandwidth of RF channel
that is engaged and is defined as,

$$B = (N_u + 1)\ x\ \Delta f \quad (16)$$

2.4 Requirements

The proposed work is based on wireless communication field and hence can easily be tested for functionalities through simulations and with the use of communication tool box functions, the desired outcome can be achieved. Hence, MATLAB is a very useful software tool. Table 2.1 and 2.2 shows the software and hardware requirements respectively.

Table 2.1: Software description.

Operating system	Windows 10
Coding Language	MATLAB
Tool	MATLAB R2014a

Table 2.2: Hardware description.

System	Intel core i3
Hard disk	1 TB
Monitor	15.6”
Input devices	Keyboard. Mouse
RAM	4GB

2.5 Flow Diagram

Figure 9 shows the flow in which the data undergoes a series of process during are transmission and reception from air to ground as well as vice versa.

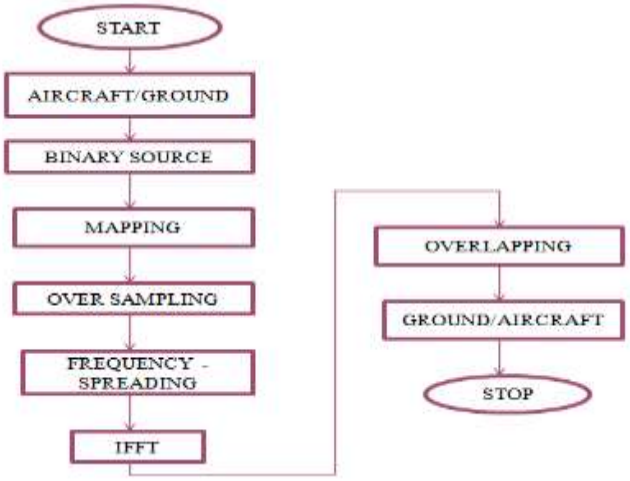

Figure 9: Flow Diagram

I. RESULTS AND OBSERVATION

This figure 10 represents the input signal that forms the first step for processing in FBMC and LDAC systems. Figure 11 shows the 3D view of the L-DACS and FBMC antennas. Figure 12 shows the PSD of L-DACS and FBMC. Figure 13 shows BER with DME interference for all future communication systems. Figure 14 shows the SIR for L-DACS and FBMC. Figure 15 shows the observation in a tabularized format.

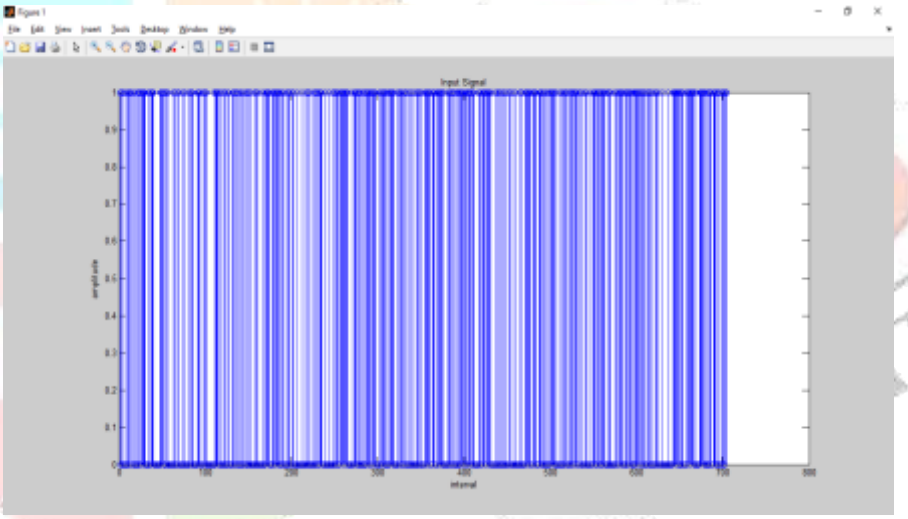

Figure 10: Input Signal

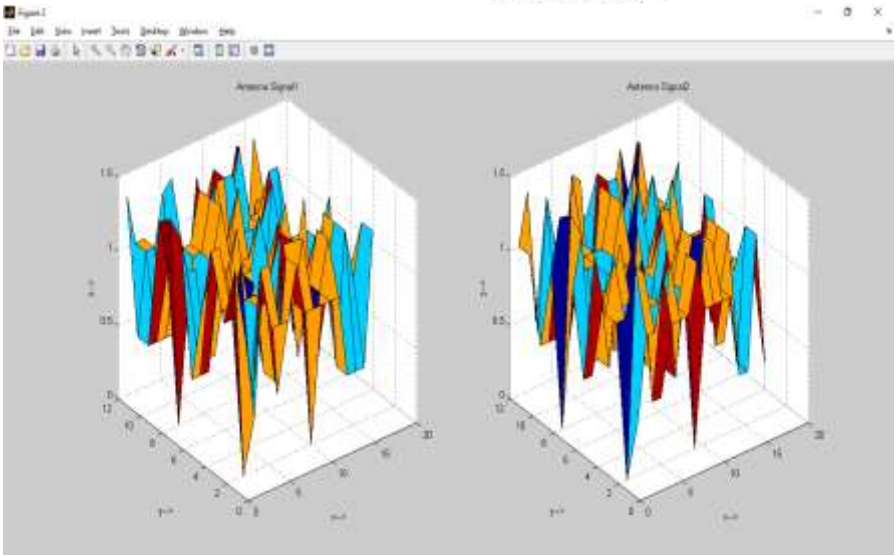

Figure 11: 3D view of L-DACS1 and FBMC antennas

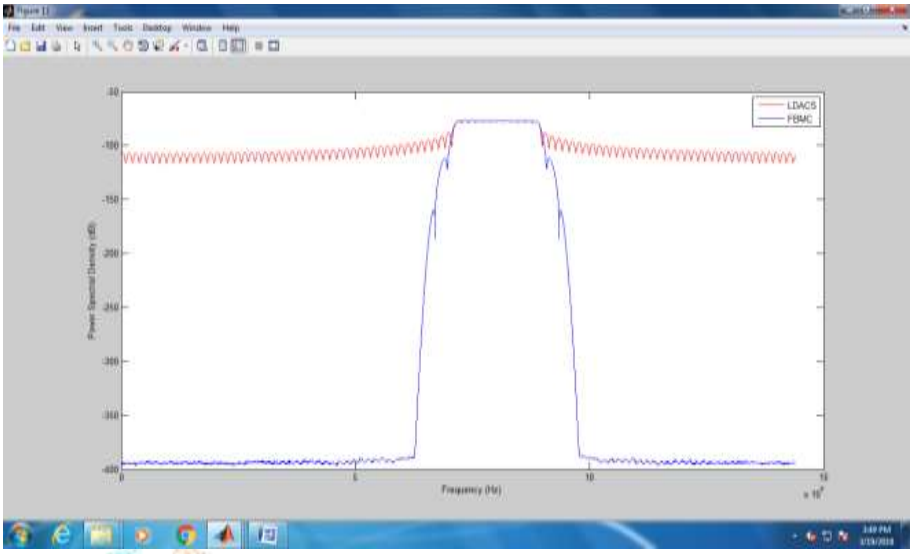

Figure 11: PSD of L-DACS and FBMC.

Figure 12: BER with DME interference.

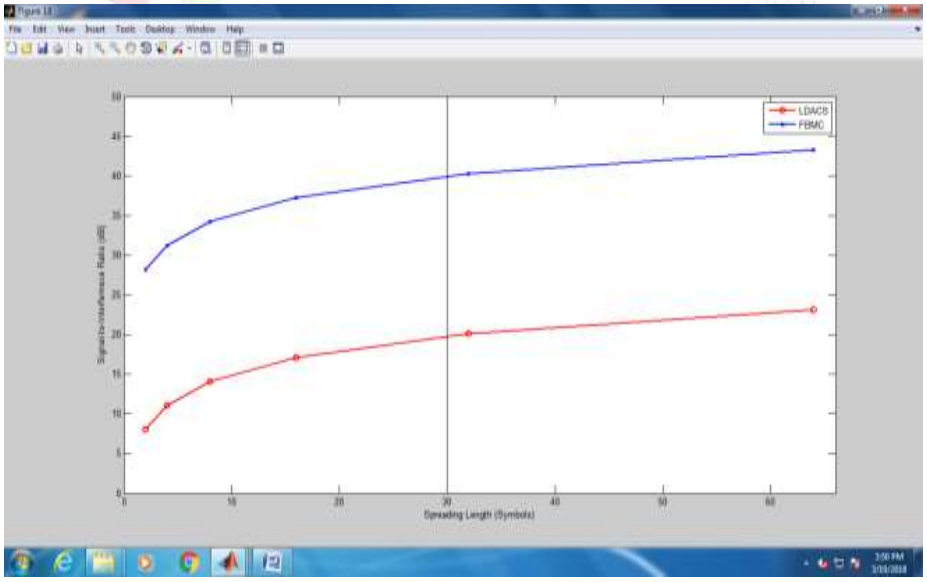

Figure 13: SIR for L-DACS and FBMC.

<table>
<tr><th colspan="2">Parameters</th><th colspan="3">L-DACS</th><th>FBMC</th></tr>
<tr><td rowspan="2">PSD</td><td>no data for transmission</td><td colspan="3">-110dB</td><td>-400dB</td></tr>
<tr><td>data present for transmission</td><td colspan="3">-80dB</td><td>-80dB</td></tr>
<tr><td rowspan="4">BER Performance</td><td rowspan="2">without DME interference</td><td>L-DACS1</td><td colspan="2">10^{-6}</td><td rowspan="2">10^{-4}</td></tr>
<tr><td>L-DACS2</td><td colspan="2">10^{-5}</td></tr>
<tr><td rowspan="2">with DME interference</td><td rowspan="2">L-DACS1</td><td>With PB</td><td>10^{-5}</td><td rowspan="2">with PB
10^{-4}- 10^{-5}</td></tr>
<tr><td>Without PB</td><td>less than 10^{-5}</td></tr>
<tr><td rowspan="2">L-DACS2</td><td>With PB</td><td>10^{-5}</td><td rowspan="2">without PB
10^{-6}</td></tr>
<tr><td>Without PB</td><td>10^{-4}- 10^{-5}</td></tr>
<tr><td colspan="2">SIR</td><td colspan="3">19dB</td><td>39dB</td></tr>
</table>

Figure 14: Observation table

II. CONCLUSION

Description and potential evaluation of the FCI candidates has been successfully achieved. From the simulation results it is evident that the interference from the Distance Measuring Equipment is rigorous for both the proposed communication systems and illustrates filter bank multicarrier is much resistant than the 1-2 GHz system used for aeronautics in the presence of Distance Measuring Equipment interference .The proposed system posses the capacity to function exclusive of Pulse Blanking and possesses finest functioning when compared to the L-DACS systems. Filter bank multicarrier systems provides improved throughput than L-DACS1 systems since subcarriers of guard band are reinstated to data and also possess low Out of Band frequency which helps in the reduction of interference to different communication systems in the L-band. Our simulation results justifies that FBMC can be considered as an appealing candidate for bandwidth spectrum of analysis for the future aeronautical communication systems. Forthcoming work involves estimating the performance of communication systems in various plots and also incorporating to perform an internal testing towards real time validation to work the mathematical certainty.

III. ACKNOWLEDGEMENT

I would like to thank Mrs. Poornima B, Assistant Professor, Atria Institute of Technology, for her constant support and help. My sincere thanks to anonymous reviewers for their valuable comments and useful suggestions.

REFERENCES

[1] N. Neji, R. De Laerda, A.Azoulay, T.Letertre, O.Outtier, “Survey on the Future Aeronautical Communication System and Its Development for Continental Communication,” IEEE Trans. Vehicular Tech., vol.62, no.1, pp.182-191, Jan2013.

[2] D.W .Matolak, R. Sun, “Air-Ground Channel Characterization for Unmanned Aircraft Systems-Part 1: Methods, Measurements, and Models for Over-water Settings,” to appear IEEE Trans. Vehicular Tech., Oct.2015.

[3] R.Sun, D.W. Matalok, “Air-Ground channel characterization for Unmanned Aircraft Systems- Part2: Hilly Mountainous Settings,” to appear, IEEE Trans.Vehicular Tech., December 2015.

[4] S.Brandes, et al. “Physical layer specification of the L-band Digital Aeronautical Communication Systems (L-Dacs1). “Integrated Communication Navigation and Surveillance Conference (ICNS), IEEE, pp.1-12, Arlington VA, 13-15 May 2009.

[5] Wenjia Cui, Daiming Qu, Tao Jiang, and Behrouz Frahang- Boroujeny, “Coded Auxillary Pilots for Channel Estimation in FBMC-OQAM systems, IEEE Trans. On Vehicular Technology, 2016.

[6] Mohamad Mostafa, Nico Franzen and Michael Schnell, “DME signal power from inlay LDACS1 perspective” German Aerospace Center DLR, Munchener Strabe 20, 822234 Webling, Germany, 2014.N.

[7] D. Kong, Xiang-Gen Xia, T. Jiang and X. Gao, “Channel Estimation in CPOQAM – OFDM systems,” IEEE Trans. On Signal Processing, vol.62, no.21, pp. 5775-5786, Nov 2014.

[8] Raj Jain Fred Templin, Kwong-Sang Yin, “Analysis of L-band Digital Aeronautical Communication Systems: LDACS1 and LDACS2,” IEEE Aerospace Conference, Big Sky, Montana, 2011.